The International Archives of the Photogrammetry, Remote Sensing and Spatial Information Sciences, Volume XLVIII-M-7-2025
44th EARSeL Symposium, 26–29 May 2025, Prague, Czech Republic

Dimension Expansion-based Spatiotemporal Land Cover Change Detection: A Study Case Using Sentinel-2 Satellite Time Series

Meng Lu

Department of Geography, University of Bayreuth

Keywords: Dimension Expansion, Sentinel-2, Satellite Image Time Series, Gaussian Process, Change Detection

Abstract

Satellite time series data enable continuous land cover change detection, classification, and monitoring across large geographical areas. Time series-based statistical methods for abrupt change detection remain widely used in understanding and monitoring environmental dynamics but face limitations, including sensitivity to noise, challenges in differentiating change classes and causes, detecting change in near real-time, and incomplete uncertainty quantification. These challenges are obvious in cultivated lands, where the seasonality and cultivated areas often alter in different years. On the other hand, change detection and classification in space-time is difficult due to the nonstationary presented in data. In this study we used dimension expansion-based approach that projects data to higher dimensionality for stationarity and understand the change of spatial stationarity over time. Our case study focuses on vegetation dynamics in a cultivated and managed terrestrial area in the Takamanda National Park in Cameroon, a protected area of significant ecological value, using Sentinel-2 satellite time series data. The results imply the possibility of new spatiotemporal approach that is robustness against noise and enables near-real-time monitoring.

1. Introduction

Monitoring abrupt land cover changes is essential for conservation and understanding the natural and antropogenic effects. Change monitoring is particularly necessary in ecologically sensitive regions, such as protected areas. Advancements in spatial, spectral, and temporal resolution of satellite time series data provide unprecedented opportunities for continuous, large-scale spatio-temporal monitoring. These advances enable the detection of critical changes such as forest degradation, deforestation, and urban expansion. Time-series-based change detection methods, such as the BFAST framework (Verbesselt et al., 2010), which is based on the empirical fluctuation process (Zeileis et al., 2007), and TrendR, which is a more empirical residual manipulation process, are widely used due to their flexibility in capturing the trend and seasonality in time series. Many variations of time-series abrupt change detection methods, including deep learning-based approaches, have been developed. However, purely time-series methods do not make full use of information from other dimensionality and have notable limitations: first, a time-series analysis approach is sensitivity to noise: Spectral variations caused by atmospheric interference can trigger false detections. Secondly, it has difficulty in differentiating change classes and causes: Relying on a single-pixel time series for change detection misses spatial patterns and does not make full use of multispectral bandinformation. On the other hand, spatiotemporal Gaussian process is attractive in detecting spatiotemporal change at once as opposed to a separated spatial-first then time approach or the opposite. However, spatiotemporal Gaussian Process (GP) is itself a significant challenge, firstly due to the composition of a valid and efficient spatiotemporal kernel, secondly due to the nonstationarity in space-time.

Quantifying spatial patterns provides important information in understanding the spatial process and the change of it. Most spatial pattern quantification methods focusing on calculating variability of a vegetation index, such as using Coefficient of Variation (CV), or the using the parameters of variograms, such as sill, range, and nuggest. However, applying these methods globally provide limited information about spatial patterns. The CV and variograms could be calculated in divided zone or moving windows. But first of all it is difficult to define such windows. More importantly, local variograms or Kriging introduce several methodological and statistical issues such as inconsistant variogram modelling, loss of spatial structure, and unreliable uncertainty quantification (Goovaerts, 1997, Haas, 1990, Journel, 1978).

Dimension expansion methods are techniques transform data into higher-dimensional spaces, where hidden structures could be revealed. The methods aligns with concepts in manifold learning. The dimension expansion technique was introduced firstly in (Sampson and Guttorp, 1992), who proposed transforming nonstationary spatial processes into a latent Euclidean space where stationarity holds. In computational age, (Bornn et al., 2012) extended this concept by formulating dimension expansion as an optimization problem, where the goal is to learn new dimensions that minimizes the discrepancy between the spatial dispersion of the observations and the variogram in the expanded space. Regularization is applied to ensure smoothness and to avoid overfitting the latent dimensions. These approaches may be particularly valuable in the application of geostatistics in understanding complex land surface patterns, which commonly do not follow the assumption of stationary.

In this study, we developed a change detection method that is based on the dimension expansion and Gaussian process. We applied our method to Sentinel-2 L2A NDVI time series in a cultivated landscape within the Takamanda National Park in Cameroon. Our goal is to 1) assess the capability of the developed method in capturing phenological phase shifts and changes between years, and 2) implement the dimension expansion approach and understand what is learned in the new dimensions and how the change informaiton could be captured. We hypothesize that with carefully selected features and objective function, the dimension expansion approahch could reflect a variety of valuable information that help distinguish temporal transitions, making it a promising tool for detecting land cover change and understanding our dynamic environments.

2. Method

2.1 Dimension Expansion

The dimension expansion method proposed by (Bornn et al., 2012) minimises the difference between spatial dispersion and the variogram in the new space with extended dimensions. The objective function can be expressed as:

$$\hat{\phi}, \hat{Z} = \arg\min_{\phi, Z'} \sum_{i<j} \left(v^*_{i,j} - r(d_{i,j}(X, Z'))\right)^2 + \lambda_1 \sum_{k=1}^{p} \|Z'_k\| \tag{1}$$

where X = the original dataset.
Z' = the learned expansion
$\hat{\phi}$ = the learned hyperparameters of the kernel function.
$v^*_{i,j}$ = the spatial dispersion between sites i and j
r = the variogram
$d_{i,j}(X)$ = the distances between i and j
$\lambda_1 \sum_{k=1}^{p} \|Z'_k\|$ = the regularization term.

The spatial dispersion $v^*_{i,j}$ is calculated as:

$$v^*_{i,j} = \sum (Y(x_i) - Y(x_j))^2 \tag{2}$$

2.2 Study area

The study area (figure 1) is in the Takamanda National Park in Cameroon, a protected area of significant ecological value. In this study, we experiment on a 1 km * 1 km area, the area is classified into cultivated and managed terrestial land based on (Szantoi et al., 2020), this can also be seen from the worldview2 image on the right.

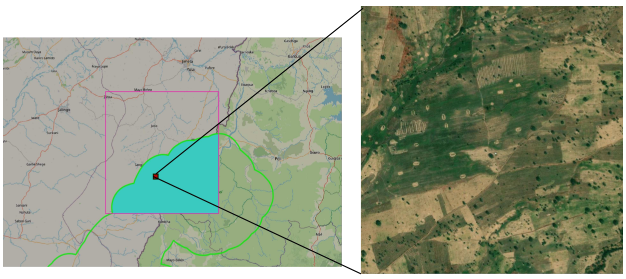

Figure 1. Study area, the magenta rectangle indicates the tile of sentinel 2 L2A image that is used. The national park is outlined in green. The red rectangle in the turquoise intersection is our study area. On the right, a timestamp of the worldview-2 image of the area is shown.

2.3 Implementation

The dimension expansion algorithm is implemented in R, using BFGS to optimise the objective function. The spatial dispersion v^* and variogram r (equation 1) are log transformed. The choice of initial values, namely the hyperparameters, and the penalty terms affect significantly the optimisation results. After experiencing with different options, we set the model as follows. When using the spatial location as features, i.e. as in Ordinary Kriging, the Matern kernel function with $\mu = 1.5$ is chosen as the variogram function; length scale is set to 10000. When using the previous time stamp as features, i.e. as in Gaussian process in general, the Gaussian kernel function is chosen as the kernel function; length scale is set to two times the maximum of the feature distances . In both cases, the variance is initiated as the variance of a single time stamp and the L1 norm penalty is set to the sum of the absolute value of the learned locations.

Several vegetation indices were explored, including the NPRB, the normalised difference between red band (band 4) and blue band (band 2); the moisture band, normalised difference between the near infrared band (band 08A) and short wave infrared band (band 11); the NDTI, the normalised differencing tillage band, and chose to use NDVI as it best represent seasonality change in the area.

To reduce the computational cost, we regularly sampled 400 locations from each image, corresponding to a sample every 5 locations. The grid sampling allows us to better understand the spatial patterns of learned locations. Note that the scaling the features could greatly increase the computational speed.

2.4 Phenological phases identification

As the dimension expansion approach aims to push locations of high variations to high values in the new dimension (so that the distances between the locations are enlarged), it could be used as a tool to assess spatial variability. Combined with vegetation index, in this study NDVI, we could design algorithms that classify scenes and identify change. In this study, we classify the following situations with algorithm design criteria on top of criteria that is only based on the magnitude and variability of a vegetation index spatially or temporally, as has been suggested in a variety of studies (Brown and Pervez, 2014, Pettorelli et al., 2005). This makes the classification or change detection more robust and less sensitive to a certain threshold based on the magnitude and a variability measure such as the CV

We carefully reviewed all false-color near-infrared (NIR) and true-color images and identified four important phenological phases (Table 1 and proposed algorithm design criteria for each of them in addition to using the magnitude and variability of NDVI in Table 2.

2.5 Phenological phases shift identification

To identify phenological phase shifts, we mainly rely on model-a: the spatial locations of the NDVI at time t ($NDVI_t$) as feature (same as in Kriging), and model-b: NDVI at time $t-1$ ($NDVI_{t-1}$) as the feature (or "location"), for $NDVI_t$. The main hypotheses are:

1. High correlation between $NDVI_t$ and learned locations using model-a indicates change from t-1 to t.
explaination: if the spatial pattern of $NDVI_{t-1}$ changes little from the $NDVI_t$, the $NDVI_{t-1}$ is a good predictor for the $NDVI_t$, and the learned locations will have a low correlation with $NDVI_t$. If there is a phenological shift, the $NDVI_{t-1}$ is not a predictor of $NDVI_t$ and the correlation between $NDVI_t$ and the learned locations will be high.

Phenological Phase	Months	Landscape Characteristics
1. Early growing season	May–Jun	Vegetation emergence with surrounding bare patches
2. Transitional shift	Jul–Aug	Vegetation expands into previously bare areas; some regions become bare again
3. Peak growth (vigorous)	Sep–Oct	Vegetation dominates the landscape
4. Wilting and senescence,	Nov- Jan	Vegetation retreats across the field
5. Dormant season	Feb–April	Wet or bare soil dominate the landscape

Table 1. Seasonal vegetation phases and landscape patterns derived from monthly imagery. Note the month is based on 2017, for other years the month could shift.

2. Low correlation between $NDVI_t$ and learned locations using model-b indicates homogeneous or smooth spatial patterns. The relative values between time indicate how spatial patterns change. To illustrate, in the phenological phases 3 (peak growth) and 5 (dormant season), the spatial locations are a good predictor of the $NDVI_t$ due to the homogeneous spatial pattern.

To prevent the effects of extreme values of learned location, the Kendall's τ is used as a non-parametric measure of correlation.

The phenological phase shift is defined by the following criteria:

- Criteria-A: the Kendall's τ between the absolute learned locations and $NDVI_t$ using $NDVI_{t-1}$ as feature.
- Criteria-B: the Kendall's τ between the absolute learned locations and $NDVI_t$ using spatial locations as feature.

Table 2 shows the algorithm design criteria, note the CV of NDVI and criteria B both provide information about variation, but Criteria-B quantifies explicitly spatial patterns. The threshold for Criteria-A is empirical for our study case and need to be tuned or automatically learned for other studies.

3. Results

The learned locations are illustrated in Figure 6. A clear distinction emerges when comparing the plots from the post-harvest and plant growing seasons in 2017. During winter, only a few locations are significantly displaced in the learned dimension, these correspond to evergreen vegetation, which stands in contrast to the majority of the region that comprises bare or wet soil. This interpretation is supported by the spatial distribution of the learned locations, along with the corresponding NDVI and false-color NIR plots shown in Figures 4 and 5. Figure 5 excludes extreme values, defined as those exceeding $1.5 \times$ IQR above the upper quartile (Q_3) or below the lower quartile (Q_1), making it easier to identify both the outliers (which are filtered out) and the more moderate values, which can then be analyzed more clearly. Figure 5 b shows that the learned locations are scattered, mostly in the vegetated areas.

In the growing season, more locations have high absolute values in the new dimension (figure 6 b). It shows an oscillatory pattern, which indicates the variation within the certain land cover class, here, bare soil and vegetation. From figure 5 c and d, we could observe a patch of bare soil surrounded by healthy vegetations. The brightest blue area (figure 5 c), which has the lowest NDVI 5, has the learned locations with the most extreme values in the new dimension, and the slightly darker area (figure 5 c) has the learned locations with less extreme but also high absolute values in the new dimension.

We move further to September 2017 and compare with September 2019 to understand the application of the dimension expansion approach in understanding within-year dynamics and and between-year change. In september 2017, the vegetation is at its full growth, note that the bare soil area in figure 5 c is also covered by vegetation. As the vegetation dominated the scene, the learned locations have extreme values mostly in bare soil areas. In comparison, in September 2019, the learned locations show higher variations, as there is less vegetation. The learned locations have higher values in vegetated areas as the bare soil is more dominating in the scene.

With both model-a (spatial locations as feature) and model-b ($NDVI_{t-1}$ as feature) We calculated the Kendall's τ correlation between learned locations and the NDVI, and found that if we remove the extreme values of the learned location using the $1.5 \times IQR$ criteria, most of the time stamp has a high Kendall's τ of 1 or above 0.85, this is especially true with model-a. This may suggest that most information is learned in the more extreme locations and the importance of using a non-parametric correlation measure instead of filtering out extreme values.

We show two examples where the phenological shift is detected. An example of a high correlation between the learned locations and NDVI using model-b is $NDVI_{t-1}$ is January 22, 2017 and $NDVI_t$ is March 23, 2017 (figure 2 a, b). The Kendall's τ is 0.9, indicating a phenological phase shift with high probability. The Kendall's τ changes from 0.22 to 0.94 using model-a from Janurary to March, showing the spatial pattern is becoming less smoother. Reflecting a spatially smooth pattern in the wilting season and the scattered vegetations of different levels of greenness, as well as soil of different levels of wetness in the dormant season.

Another example of a relatively lower but still high correlation between learned location and the NDVI using model-b is from August to September, 2017 (figure 2 c and d), the Kendall's τ = 0.68, indicating a phenological phase shift with medium probability. The Kendall's τ changes from 0.83 to 0.68 using model-a from August to September 2017, showing the spatial pattern is becoming smoother. This is reasonable that when the plant is in full-growth, the spatial correlation increases.

Then, we show two examples where no phenological shift is indicated. One is from January to April, 2020, the learned locations using model-b (figure 3 show a very low correlation (Kendall's τ = -0.04) with NDVI. The Kendall's τ changes from 0.94 (Januaray) to 0.6 (April) using model-a, showing the spatial pattern is becoming smoother. Another example is from September to October, 2020 (figure 3 c and d). The Kendall's τ is 0.11, indicating no phenological phase shift with high probability. The NDVI and learned locations are perfectly correlated using model-a, indicating no spatial patterns. Compared to the example above for 2017, we could also identify a seasonality change from 2017 to 2020 - the spring comes late in 2020.

Phase shifting	Criteria
1 -2	Criteria-A >0.6; Criteria-B stays or slightly decrease
2 -3	Criteria-A >0.6; Criteria-B decreases, NDVI increases, CV of NDVI decreases
3 -4	Criteria-A>0.6; Criteria-B increases, NDVI decreases, CV of NDVI decreases
4 -5	Criteria-A> 0.8; Criteria-B increases, NDVI decreases, CV of NDVI increases
5 -1	Criteria-A> 0.8; Criteria-B decreases, NDVI decreases, CV of NDVI decreases

Table 2. Algorithm design criteria for detecting phenological phase shifting. A and B are the criteria defined above. CV: Coefficient of Variance .

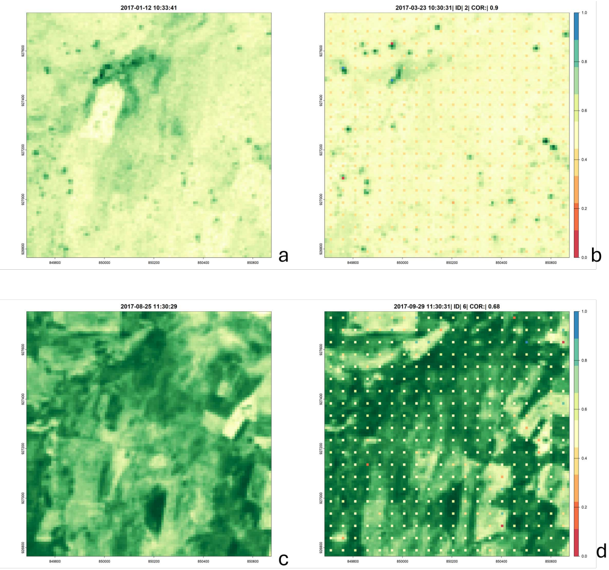

Figure 2. Learned locations using model-b ($NDVI_{t-1}$ as feature). The learned locations show a high correlation (b) and medium correlation (d) with the NDVI, indicating a phenological phase shift with respectively higher and lower probability.

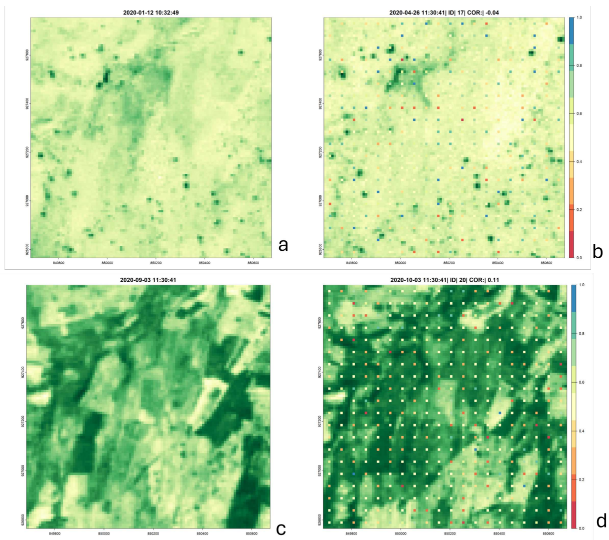

Figure 3. Learned locations using model-b ($NDVI_{t-1}$ as feature). The learned locations show a very low correlation (b) and low correlation (d) with the NDVI, indicating no phenological phase shift with high probability.

4. Discussion

In this study, we applied dimension expansion to satellite image time series from the Sentinel-2 L2A product to understand changes in a cultivated land area within Takamanda National Park in Cameroon. This approach provides an efficient means of interpreting spatial patterns, phenological phase shifts, and inter-annual changes. The learned dimension captures the spatial heterogeneity of the region and highlights areas of distinction within the imagery, such as vegetation during the dormant season or bare soil in vegetated areas. By analyzing the correlation between the learned locations and the observations, using different features, valuable information on temporal change and spatial smoothness can be revealed. The proposed method has the potential to detect both phenological phase shifts and changes in seasonality or land cover across years. It may also be applied to more accurately delineate the expansion of phenomena such as fire or specific vegetation species.

When using the sspatial locations are features, as in Kriging, it was found that without the extreme values, the learned locations are oftentimes the NDVI itself. The learned locations with extreme values are usually locations that have a distinctive NDVI values in the scene. However, if we only looking at the NDVI values of a few locations, we are unable to know how these values compare to the other locations of the image. One can calculate the percentile of each location, but this does not allow the incorporation of the spatial information. The causes of the issue is mainly due to the feature used. If the feature is a poor predictor, the learned locations will have very high correlations with the observations, or even being the observation itself. If the feature is a good predictor, more meaningful knowleage will be learned in the expanded dimension. It is also possible to modify the objective function to prevent the learned dimension to copy the observations.

The objective function proposed in (Bornn et al., 2012) tries to fit a kernel using distances in the new dimensional space, this will push the locations of extreme values far away with a large length scale, as the increment of the kernel function slows down tremendously if an exponential function is used. This explains the extreme values in the learned locations and why removing them result in high correlation with NDVI. his suggests the importance of choosing objective functions, kernels and regulation, while the original aim of (Bornn et al., 2012) is to bring data to higher dimensions so that the stationarity assumption is guaranteed. Note that is it the nature and risk of such optimisation methods that the learned dimensions do not necessarily have physical meanings. The hope is that it could however magnify change signals and extract interesting patterns.

Note that even though theoretically, the stationarity is guaranteed in the high dimensional space, due to the optimisation path and the number of expanded dimensions, the variogram might not be successfully learned in the expanded space. Figure 7 shows the variograms in the new space (a and b) and the original space (c and d) for the January and June images in 2017, respectively. It can be observed that the variogram for the 06.2017 image shows more spatial pattern compared to the original, but the variogram for the 01.2017 image is less successful. Regardless of a successfully learned variogram, the expanded dimension aims at pushing values with high spatial variability, or low spatial covariance, to a high absolute value in the new dimensions. If the variogram is learned successfully, the meaning of the expanded space is clearer and our analysis is more reliable. Thus, the variogram in the learned space could serve as an uncertainty measure of our method.

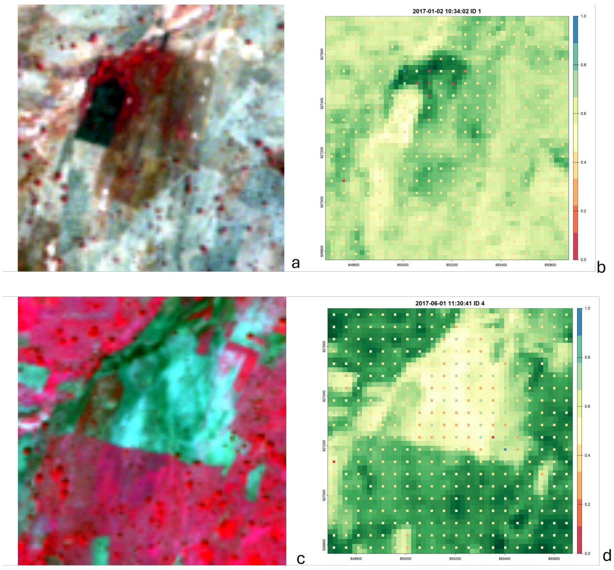

Figure 4. The learned locations of two different time stamps, in Januaray and June, 2017, respectively. The min-max normalization is applied to the learned locations. The base map is the NDVI (normalised difference vegetation index) map, the legend of which is not shown as the absolute value is not important. The greener, the higher the NDVI value and the whitish, the opposite. a and c are false-color Near-infrared maps, i.e., the RGB composition of bands near-infrared, red, and green.

5. Conclusion

In this study, we implemented and applied a dimension expansion-based method to Sentinel-2 L2A NDVI time series over a cultivated terrestrial landscape within a conservation region in Cameroon to identify phenological phase shifts as well as between-year changes. We defined phenological phases and analyzed the behavior of the learned dimension using different features. We found that the predictor and objective function play important roles in this approach. Using spatial coordinates as features could tell us the change in spatial patterns, while using the previous time stamp as features could tell us about change. The value of this work lies not only in the implementation of the dimension expansion approach, but also in exploring its capacity to characterize spatial heterogeneity and temporal transitions. Our findings highlight its conceptual promise. Future work incorporating multiple learned dimensions, alternative objective functions, meaningful features, and different regularization strategies could improve the robustness and interpretability of this method. We could show that the dimension expansion is a promising technique for extracting structure from spatial-temporal data and this work lays the foundation for further methodological development in the quantification and monitoring of our dynamic and complex environment.

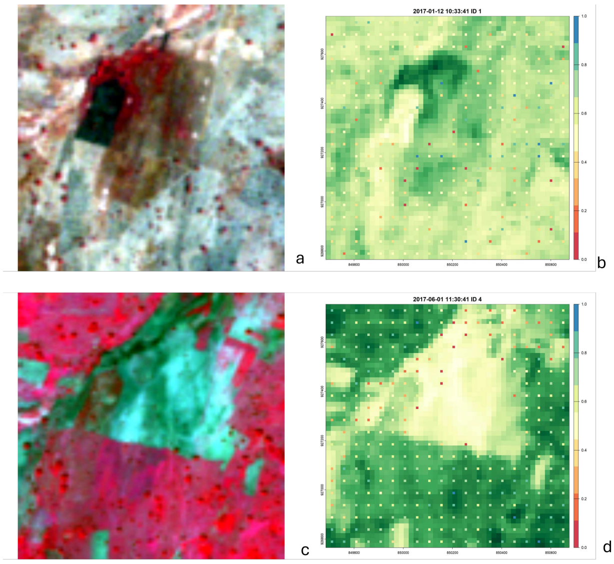

Figure 5. The learned locations of two different time stamps, in Januaray and June, 2017, respectively, with the extreme value of 3 IQR removed for visualisation, i.e. Lower Bound: (Q1 - 3 * IQR) Upper Bound: (Q3 + 3 * IQR). The min-max normalization is applied to the learned locations. The base map is the NDVI (normalised difference vegetation index) map, the legend of which is not shown as the absolute value is not important. The greener, the higher the NDVI value and the whitish, the opposite. a and c are false-color Near-infrared maps, i.e., the RGB composition of bands near-infrared, red, and green.

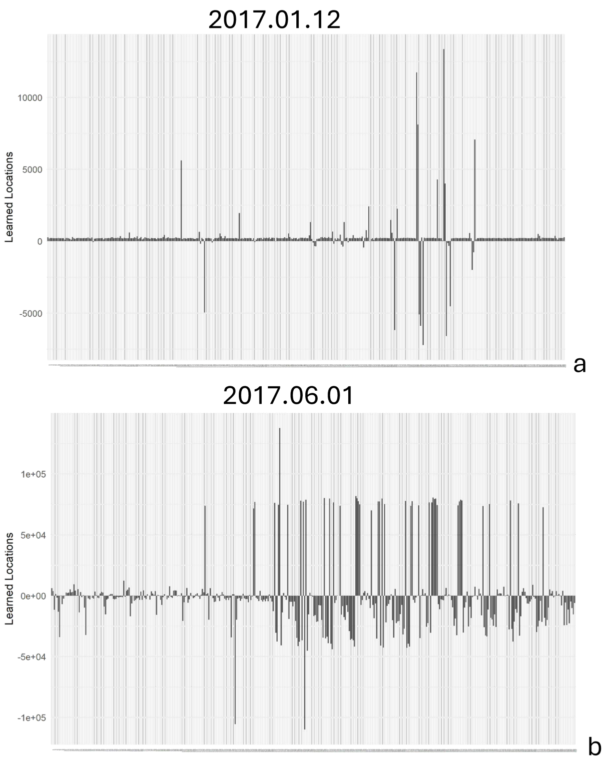

Figure 6. Learned locations. The x-axis is sorted by the location index, starting from the lower left corner. For two time stamps.

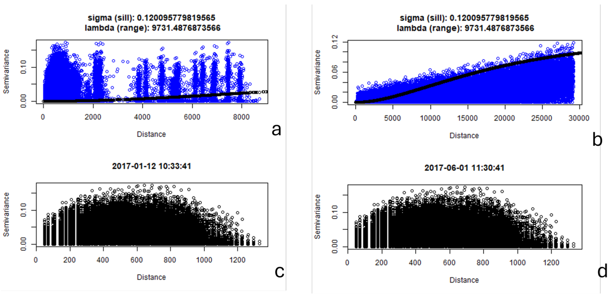

Figure 7. The variogram in the learned space (upper figures) and the original space (lower figures). The cut-off is set to the three times length scale for the learned space.

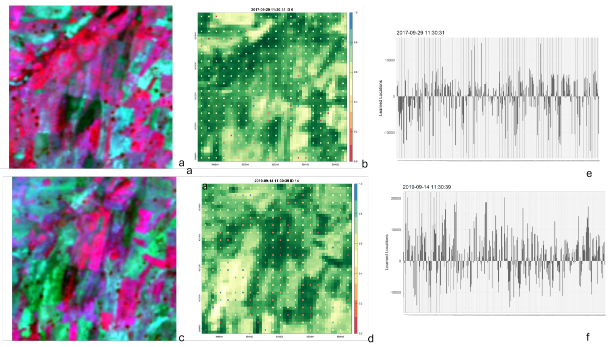

Figure 8. The learned locations of two different time stamps, in september 2017 and 2019, respectively. The min-max normalization is applied to the learned locations. The base map is the NDVI (normalised difference vegetation index) map, the legend of which is not shown as the absolute value is not important. The greener, the higher the NDVI value and the whitish, the opposite. a and c are false-color Near-infrared maps, i.e., the RGB composition of bands near-infrared, red, and green. e and f shows the learned locations on y-axis, with the x-axis is sorted by the location index, starting from the lower left corner.

References

Bornn, L., Shaddick, G., Zidek, J. V., 2012. Modeling non-stationary processes through dimension expansion. *Journal of the American statistical association*, 107(497), 281–289.

Brown, J. F., Pervez, M. S., 2014. Merging remote sensing data and national agricultural statistics to model change in irrigated agriculture. *Agricultural Systems*, 127, 28–40.

Goovaerts, P., 1997. *Geostatistics for natural resources evaluation*. Oxford university press.

Haas, T. C., 1990. Kriging and automated variogram modeling within a moving window. *Atmospheric Environment. Part A. General Topics*, 24(7), 1759–1769.

Journel, A., 1978. *Mining geostatistics*. Academic Press.

Pettorelli, N., Vik, J. O., Mysterud, A., Gaillard, J.-M., Tucker, C. J., Stenseth, N. C., 2005. Using the satellite-derived NDVI to assess ecological responses to environmental change. *Trends in ecology & evolution*, 20(9), 503–510.

Sampson, P. D., Guttorp, P., 1992. Nonparametric estimation of nonstationary spatial covariance structure. *Journal of the American Statistical Association*, 87(417), 108–119.

Szantoi, Z., Brink, A., Lupi, A., Mannone, C., Jaffrain, G., 2020. Key landscapes for conservation land cover and change monitoring thematic and validation datasets for sub-Saharan Africa. *Earth System Science Data Discussions*, 2020, 1–28.